Hydrol. Earth Syst. Sci., 15, 3577–3589, 2011
www.hydrol-earth-syst-sci.net/15/3577/2011/
doi:10.5194/hess-15-3577-2011

Hydrology and Earth System Sciences

The sensitivity of land emissivity estimates from AMSR-E at C and X bands to surface properties

H. Norouzi[1, 2, *], **M. Temimi**[2], **W. B. Rossow**[2], **C. Pearl**[2], **M. Azarderakhsh**[1, 2], **and R. Khanbilvardi**[2]

[1]Graduate Center of the City University of New York, New York, USA
[2]City College of the City University of New York / NOAA-CREST, New York, USA
[*]now at: New York City College of Technology, The City University of New York, New York, USA

Received: 19 May 2011 – Published in Hydrol. Earth Syst. Sci. Discuss.: 14 June 2011
Revised: 7 November 2011 – Accepted: 12 November 2011 – Published: 25 November 2011

Abstract. Microwave observations at low frequencies exhibit more sensitivity to surface and subsurface properties with little interference from the atmosphere. The objective of this study is to develop a global land emissivity product using passive microwave observations from the Advanced Microwave Scanning Radiometer – Earth Observing System (AMSR-E) and to investigate its sensitivity to land surface properties. The developed product complements existing land emissivity products from SSM/I and AMSU by adding land emissivity estimates at two lower frequencies, 6.9 and 10.65 GHz (C- and X-band, respectively). Observations at these low frequencies penetrate deeper into the soil layer. Ancillary data used in the analysis, such as surface skin temperature and cloud mask, are obtained from International Satellite Cloud Climatology Project (ISCCP). Atmospheric properties are obtained from the TIROS Operational Vertical Sounder (TOVS) observations to determine the small upwelling and downwelling atmospheric emissions as well as the atmospheric transmission. A sensitivity test confirms the small effect of the atmosphere but shows that skin temperature accuracy can significantly affect emissivity estimates. Retrieved emissivities at C- and X-bands and their polarization differences exhibit similar patterns of variation with changes in land cover type, soil moisture, and vegetation density as seen at SSM/I-like frequencies (Ka and Ku bands). The emissivity maps from AMSR-E at these higher frequencies agree reasonably well with the existing SSM/I-based product. The inherent discrepancy introduced by the difference between SSM/I and AMSR-E frequencies, incidence angles, and calibration has been assessed. Significantly greater standard deviation of estimated emissivities compared to SSM/I land emissivity product was found over desert regions. Large differences between emissivity estimates from ascending and descending overpasses were found at lower frequencies due to the inconsistency between thermal IR skin temperatures and passive microwave brightness temperatures which can originate from below the surface. The mismatch between day and night AMSR-E emissivities is greater than ascending and descending differences of SSM/I emissivity. This is because of unique orbit time of AMSR-E (01:30 a.m./p.m. LT) while other microwave sensors have orbit time of 06:00 to 09:00 (a.m./p.m.). This highlights the importance of considering the penetration depth of the microwave signal and diurnal variability of the temperature in emissivity retrieval. The effect of these factors is greater for AMSR-E observations than SSM/I observations, as AMSR-E observations exhibit a greater difference between day and night measures. This issue must be addressed in future studies to improve the accuracy of the emissivity estimates especially at AMSR-E lower frequencies.

Correspondence to: H. Norouzi
(hnorouzi@citytech.cuny.edu)

1 Introduction

At lower frequencies, passive microwave observations are less affected by the atmosphere and are more sensitive to the surface and subsurface properties like soil moisture and soil texture (Choudhury, 1989, 1993). Because of this greater sensitivity and a greater penetration depth, land emissivity estimates at these lower frequencies are appropriate for applications like soil moisture estimation, freeze/thaw state, land surface temperature, and vegetation structure (e.g. Zhang et al., 2010; Tedesco and Kim, 2006; Min et al., 2010; Njoku

et al., 2003; Jones et al., 2007). In addition, land emissivity values at higher frequencies near the window regions can be extrapolated to microwave sounding frequencies to provide the critical boundary condition in numerical weather prediction (NWP) models (Weng et al., 2001; Karbou et al., 2005a). Interpretation of microwave emissivity over land is not very straightforward as it is affected by several factors such as soil wetness and roughness, vegetation cover, macroscopic mixtures of vegetation, soil and rock, and terrain slopes, as well as sensor properties (i.e. frequency, polarization, and incidence angle).

Land emissivity has been retrieved globally since the 1990's from different sensors such as the Special Sensor Microwave Imager (SSM/I) and the Advanced Microwave Sounding Unit (AMSU) at frequencies greater than or equal to 19 GHz. Choudhury (1993) used observations from SSM/I to investigate the inter-annual variation of land surface microwave reflectivity (reflectivity = 1-emissivity) and suggested that it could be a good surrogate for changes in soil moisture and vegetation cover. Prigent et al. (1997, 1998, 2006) used SSM/I observations to estimate land emissivity. Their technique was extended to observations from the Advanced Microwave Sounding Unit (AMSU) (Karbou et al., 2005b). They found good consistency between land emissivity and surface properties such as soil moisture and vegetation cover type. Jones et al. (1997, 2004) also estimated land emissivity from AMSU observations. Overall consistency was found between the spatial distribution of the emissivity values obtained with SSM/I and AMSU and the global land cover-land use maps (Karbou et al., 2006). These findings were in line with those obtained from forward modeling of land emissivity. AMSR-E emissivities for frequencies higher than 10.7 GHz was estimated using MODIS skin temperature product (Moncet et al., 2011a). Weng et al. (2001) and Weng (2007) used a two-stream radiative transfer model for different land cover types to infer land emissivity and noted the complexity of modeling land emissivity over some surface classes like snow covered soils, sea ice and deserts. Land emissivity estimates at higher frequencies (higher than 19 GHz) are sensitive only to the topsoil layer, of the order of few millimeters, depending on the soil wetness, texture and frequency, and vegetation cover. Measurements at these frequencies are therefore not as useful as lower frequencies to infer subsurface parameters (Njoku et al., 2003).

The Advanced Microwave Scanning Radiometer – Earth Observing System (AMSR-E) sensor has two channels at 6.925 and 10.65 GHz (the C and X bands) beside those available onboard SSM/I. These channels penetrate deeper and are more sensitive to the surface and subsurface. Also, this sensor is on a polar orbiting satellite with different overpass times in early afternoon and morning (01:30 a.m./p.m.), as compared with most SSM/I overpass times between 06:00 to 09:00 (a.m./p.m. LT). Since the AMSR-E overpass time is closer to maxima and minima temperature of the day, the contrast between early morning and early afternoon measurements might be used to infer surface and subsurface properties: the early morning (01:30 am) observation occurs when the soil temperature profile tends to be more nearly uniform within the sensed soil layer and the afternoon observation occurs when the temperature difference between the skin and deeper layers is large (Njoku et al., 2003). When combined with other microwave sensors, such as SSM/I and WindSat, the AMSR-E measurements could also provide a better characterization of the diurnal temperature cycle.

The spatial resolution of AMSR-E lower frequencies is coarser compared to frequencies higher than 19 GHz. AMSR-E data analysis has revealed that the C and X bands are contaminated with Radio Frequency Interference (RFI) especially over US, the Middle East, and Europe. This RFI contamination problem can reduce the value of C- and X-band measurements. A spectral difference technique has been developed for AMSR-E and WindSat to quantify the RFI magnitude and extent over the US and at global scale (Li et al., 2006; Njoku et al., 2005).

Microwave emissivity is needed to improve the development of physically based precipitation retrievals over land under all weather conditions such as clear, cloudy and precipitating sky from 10–190 GHz. Related studies suggest that significant differences exist among different available products (Y. Tian, personal communication, 2011.) and more information spectrally and temporally are needed to obtain a reliable surface contribution over land in passive microwave observations.

The objective of this work is twofold; (1) first, develop a global land emissivity product using AMSR-E data over more than six years (June 2002 to June 2008) at all frequencies. The result of this study adds to the existing land emissivity products from SSM/I and AMSU and provides land emissivity estimates at two lower frequencies, the 6.9 and 10.7 GHz. (2) Second, investigate the sensitivity of the land emissivity estimates to changes in land surface conditions with a particular emphasis on the lower frequencies and their sensitivity to surface properties. The AMSR-E-based product is compared to estimates of land emissivity from SSM/I after accounting for the inherent differences between the sensors (incident angles and frequencies). A sensitivity analysis is also conducted to assess the effect of uncertainties in the inputs to the emissivity retrieval on the accuracy of emissivities. In addition, this study investigates the differences between day and night retrieved emissivities from AMSR-E and compares it to the differences obtained with SSM/I estimates.

2 Land surface emissivity calculation and data sets

The algorithm adopted to determine land emissivities in this study is similar to the approach proposed by Prigent et al. (1997, 1998). Although the approach was initially tested using SSM/I observations the algorithm is expandable

to lower frequencies as well. Few adjustments are needed, however, to account for minor differences in incidence angles, spatial resolution, and channel frequencies.

2.1 Theory

Assuming that land surface is flat and specular and considering the atmosphere as a non-scattering plane-parallel medium, the emissivity can be written as:

$$\varepsilon_{(p,\upsilon)} = \frac{T_{b_{(p,\upsilon)}} - T_{atm}^{\uparrow} - T_{atm}^{\downarrow} e^{-\tau(0,H)/\mu}}{e^{-\tau(0,H)/\mu}(T_s - T_{atm}^{\downarrow})} \quad (1)$$

where $\varepsilon_{(p,\upsilon)}$ and $T_{b_{(p,\upsilon)}}$ are the land surface emissivity and the measured brightness temperatures at polarization "p" (horizontal, "H", or vertical, "V") and frequency υ, respectively. T_s is the skin temperature and $T_{atm}^{\downarrow}$ and $T_{atm}^{\uparrow}$ are the downwelling and upwelling brightness temperatures from the atmosphere, respectively:

$$T_{atm}^{\downarrow} = \int_H^0 T(z) \cdot [\alpha(z)/\mu] \cdot e^{-\tau(z,0)/\mu} dz \quad (2)$$

$$T_{atm}^{\uparrow} = \int_0^H T(z) \cdot [\alpha(z)/\mu] \cdot e^{-\tau(z,H)/\mu} dz \quad (3)$$

In these equations, $T(z)$ is the atmospheric temperature profile, $\alpha(z)$ the atmospheric absorption at altitude z, μ the cosine of incidence angle and τ the atmospheric extinction between two altitudes which is written as:

$$\tau(z0, z1) = \int_{z0}^{z1} \alpha(z) dz \quad (4)$$

The implementation of this algorithm requires an accurate characterization of the atmospheric temperature and humidity to determine atmospheric transmissivity. Another key parameter is the thermal skin temperature. The following section describes the data sets needed for the implementation of the approach.

2.2 Data sets

2.2.1 AMSR-E microwave brightness temperatures

AMSR-E is a twelve-channel, six-frequency, total power passive-microwave radiometer system. It measures brightness temperatures at 6.925, 10.65, 18.7, 23.8, 36.5, and 89.0 GHz (Njoku and Li, 1999). Vertically and horizontally polarized measurements are made at all frequencies. The Earth-emitted microwave radiation is collected by an offset parabolic reflector 1.6 m in diameter that scans across the Earth along an imaginary conical surface, maintaining a constant Earth incidence angle of 55°. The spatial resolution of the individual measurements varies from 5.4 km at 89.0 GHz to 56 km at 6.9 GHz. AMSR-E/Aqua L2A Global Swath Spatially-Resampled Brightness Temperatures (both ascending and descending) are used for the analysis and obtained from National Snow and Ice Data Center (NSIDC). Higher frequency observations are resampled to match the lower frequencies spatial resolution. For each frequency, we select the resampled data having the closest location to the original satellite footprint and re-project these footprints to a 0.25° (at equator) equal area grid.

2.2.2 Ancillary data sets

Satellite infrared-visible-based products from the International Satellite Cloud Climatology Project (ISCCP) provide cloud cover and surface skin temperatures. The ISCCP-DX data provides information every 3 h since 1983 at a ∼30 km spatial resolution, based on merged observations from geostationary and polar-orbiting satellites (Rossow and Schiffer, 1999). The ISCCP quantities were chosen for the satellite view closest to nadir from among all available results and resampled to match the 0.25° equal area grid adopted for the passive microwave observations. The infrared-based skin temperatures represent the top surface temperature, which can be the top of very dense vegetation canopies or a mix of canopy and soil temperatures for less dense vegetation.

The TIROS Operational Vertical Sounder (TOVS) dataset available with ISCCP (Rossow and Schiffer, 1991) provides global information on air temperature and water vapor profiles at 9 vertical layers ranging from the surface to 1 mb pressure. These profiles are available on a daily basis. We assume that the impact of diurnal variations on the observed brightness temperature is minimal. Data are originally available in a 280 km equal area map but are regridded to coincide with the AMSR-E data. These atmospheric parameters are used to calculate the upwelling and downwelling brightness temperatures, as well as the atmospheric transmission. The uncertainties in atmospheric information especially TOVS data set are 2–4 K for air temperature and 20–25 % for atmospheric column precipitable water below the 300 hPa level (Zhang et al, 2006). TOVS data may include climatological values when actual measures are missing which can introduce an error in the atmospheric corrections (Prigent et al, 1998). TOVS data were selected in this study to be consistent with ISCCP products such as skin temperature, which is also based on TOVS data (See Zhang et al., 2006 for comparisons of the TOVS product with other atmospheric datasets).

For evaluation of the retrieved emissivities, the microwave land surface emissivity data set provided by Prigent et al. (2006) is used. This data set was obtained for 1993–2008 using the Special Sensor Microwave/Imager (SSM/I) observations, along with ISCCP-DX data (skin temperature and cloud cover), and NCEP Reanalysis data (Kalnay et al., 1996) (for atmospheric corrections) for its retrieval. Emissivities at 19.35, 37.0 and 85.5 GHz in both horizontal and vertical polarizations, and the 22.235 GHz sampled in the vertical only, are available in monthly composite maps.

2.3 Determination of AMSR-E land surface emissivities

AMSR-E overpass times are near 01:30 am (ascending) and 01:30 p.m. (descending) local time at the equator. Since skin temperatures from ISCCP-DX data are available every 3 h, microwave and thermal observations are not necessarily coincident. Therefore, a Spline interpolation between the eight available skin temperature measurements every day is used to infer the complete skin temperature diurnal cycle. The Spline method can estimates the daily maxima and minima that can occur between two 3-hourly samples (Aires et al., 2004). Actual acquisition time for each microwave pixel at each swath is used in the Spline interpolation to estimate more accurately the physical temperature. This may be critical in arid regions where the temperature diurnal cycle has much larger amplitude. Also, if either of two consecutive (before and after AMSR-E acquisition times) cloud flags indicates cloudy conditions, the microwave pixel is flagged as cloudy.

The upwelling and downwelling atmospheric emissions are estimated using the Liebe's MPM model to determine the atmospheric absorption (Liebe et al., 1993). Upwelling and downwelling brightness temperatures, as well as atmospheric transmission, are calculated using Eqs. (2), (3), and (4) for the AMSR-E incidence angle of 55°. Atmospheric corrections are applied to the ascending and descending overpasses. Because of the TOVS daily resolution, the same atmospheric profiles are used to correct atmospheric effects for both the ascending and descending overpasses.

Monthly composite emissivity maps are created for each frequency and polarization from the instantaneous cloud-free land surface emissivity maps. In the case of persistent cloud (longer than 30 d, which is possible in some tropical locations), land emissivity is not retrieved.

3 Land emissivity sensitivity analysis and evaluation

3.1 Sensitivity analysis

The inputs to the retrieval (skin temperature, column water vapor and brightness temperature) were tested to determine the sensitivity of the emissivity retrieval to errors in these parameters. The uncertainty in the atmospheric water vapor profile can be as much as 20–25 % (English, 1995; Lin and Rossow, 1994; Zhang et al., 2006). The sensitivity of the retrieved emissivity to the atmospheric water vapor was assessed by introducing biases into the atmospheric profile and determining their impact on the emissivity. A constant increase of 5, 10, and 25 % was applied globally to the water vapor profiles. The sensitivity was assessed for all AMSR-E frequencies. The results (Table 1) show that the sensitivity of land emissivity to water vapor errors decreases as frequency decreases. Sensitivity at C- and X-bands is the smallest. A 25 % change in water vapor leads to a global mean 0.0016 change of emissivity at 6.9 GHz and 0.03 at 89.0 GHz. The amount of the water vapor is much larger near the equator compared with higher latitudes. Therefore, the effect of the water vapor errors on emissivity retrievals is greater in the tropics and arid regions close to the equator. Moreover, given the seasonal variation of water vapor, larger errors are expected in summer than in winter. These results are similar to the test results for SSM/I (Prigent et al., 1997).

Table 1. Sensitivity of the emissivity retrieval in terms of global average change of emissivity (horizontal polarization) to 5, 10, and 25 % increase in water vapor profile.

	Variability in global mean emissivity				
Changes implemented	6.9 GHz	10.7 GHz	18.7 GHz	36.5 GHz	89 GHz
+5 %	0.00034	0.0006	0.0013	0.0029	0.0063
+10 %	0.00065	0.0012	0.0025	0.0057	0.0127
+25 %	0.0016	0.003	0.0063	0.0145	0.0323

The physical skin temperature plays an important role at lower frequencies, since the microwave radiation is more sensitive to the surface than to the atmosphere. Recent studies show that available global skin temperatures have significant differences, generally only a few degrees but up to 20 K in deserts (Jimenez et al., 2011). ISCCP skin temperature has some uncertainties that tend to increase as temperature increases. The recent study shows that root mean square (rms) differences between ISCCP and MODIS skin temperature could be 5 K and 2.5 K for day and night, respectively (Moncet et al., 2011b). However, in this study the ISCCP-DX product was used because it has a fine temporal resolution (3 hourly). This allows us to better characterize the diurnal cycle and address the differences between day and night estimated emissivities which one of the main goal of this study. The relationship between emissivity and physical skin temperature from thermal infrared is reciprocal according to Eq. (1). The sensitivity analysis showed that the difference in global mean emissivity retrieval could be as much as 0.025 for skin temperature differences of 5 K. Therefore, at lower frequencies, skin temperature is the most important source of inaccuracy. Although possible biases in skin temperatures from ISCCP can affect the absolute emissivity value, its effect on emissivity variability should not be significant during the AMSR-E period because the ISCCP results are homogeneous in quality over this time period (Zhang et al., 2006).

The uncertainty of microwave instrument calibration and its effect on the emissivity retrieval are similar to results from previous studies (Prigent et al., 1997; Karbou et al., 2005b). For instance, a 3 K decrease in observed brightness temperature leads to 0.01 decrease of emissivity at 36.5 GHz (horizontal polarization). The absolute accuracy of AMSR-E brightness temperatures has been reported as 1.0 K (Kawanishi et al., 2003), therefore T_b biases will not significantly affect the accuracy of emissivity retrieval.

3.2 Comparison to the SSM/I product

We evaluate our AMSR-E emissivity product by comparing it with the SSM/I-based emissivity product (Prigent et al., 2006) at three frequencies (19.35, 37.0, and 85.5 GHz). The common channels between AMSR-E and SSM/I have small differences in their spectral responses and incidence angles: AMSR-E frequencies are centered at 18.7, 36.5, and 89.0 GHz with an incidence of angle 55° compared to 53° for SSM/I. Moreover, the overpass times of both sensors do not match. It is necessary to accurately determine the systematic discrepancies introduced by these differences.

The radiative transfer model (RTM) described in section 2.1 was used to assess the effect of the differences in the viewing geometry and frequency. Simulated brightness temperatures at 37 and 36.5 GHz (also between 18.7, 19.35 GHz, and 89, 85.5 GHz) with the 2° difference in incidence angle (55° for SSM/I and 53° for AMSR-E incident angle) were compared by using the same skin temperature, atmospheric air temperature, and water vapor profiles. Skin temperatures coincident with the descending orbits of AMSR-E for July 2005 were used in order to minimize the effect of the diurnal cycle. Emissivities for AMSR-E and SSM/I observations were estimated using aforementioned algorithm. The model was forced by the monthly mean emissivity at descending overpass for SSM/I frequencies and incidence angle. SSM/I emissivities were retrieved with the exact model and information used in this study for the AMSR-E descending overpass. The global mean difference between two simulated brightness temperatures at 37 GHz horizontal polarization is 0.3 K with a standard deviation of 6.5 K. One should note that emissivity by itself is angular dependent, therefore part of the brightness temperature differences are related to this differences (Prigent et al., 2008). This simulated brightness temperatures difference can be translated to emissivity difference between AMSR-E and SSM/I sensors due to geometry and frequency difference.

SSM/I derived emissivities (Prigent et al., 2006) are compared with our AMSR-E product after removing the differences caused by geometry and frequency. Figure 1 shows histograms of the differences at 18.7, 36.5, and 89.0 GHz (horizontal polarization). The mean and standard deviation of the differences between the two products are respectively 0.006 and 0.0225 (at 36.5 GHz, horizontal polarization), which indicates good agreement. The mean and standard deviation of the differences between both emissivity products (at 36.5 GHz, horizontal polarization) are respectively 0.0061 and 0.031 without accounting for differences in geometry and frequencies. The largest differences appear in arid and mountainous locations. The differences in mountainous locations can be attributed to differences in the fields of view of these sensors. Topographic features and the presences of mountainsides may amplify the effect of the difference in fields of view with respect to flat prairies-like areas. No altitude effect correction has been done for atmospheric corrections in mountainous regions. The TOVS profiles are properly terminated over high terrain but only approximately as the topographic variability is smaller scale that the available surface pressure information; nevertheless, there is much less atmospheric effect over high terrain because the column water vapor amounts are much smaller. No adjustment has been done for atmospheric corrections in mountainous regions to account for the altitude and its effect on temperature and water vapor profiles. The differences in arid regions may be caused by the difference in overpass times and the difference of the diurnal temperature cycle amplitude at the surface and at deeper layer below surface (Prigent et al., 1999). This difference is exaggerated at the AMSR-E overpass times as compared to the SSM/I overpass times near dawn and dusk. In coastal areas, the different spatial resolutions can produce large differences as well because of mismatch in the amounts of open water included in the field of view of each sensor. The bias at 89.0 GHz can be attributed to differences between the two different atmospheric correction data sets (Zhang et al., 2006), as the effect of atmosphere is larger at higher frequencies. The SSM/I-based emissivity product used the NCEP reanalysis (Kalnay et al., 1996) for atmospheric information, while this study used the TOVS product. The SSM/I based emissivity made use of the TOVS data set as atmospheric information in its first version to correct for the atmospheric effect (Prigent et al., 1997). NCEP reanalysis atmospheric profiles were used in subsequent version because of some flaws that were noticed in SSM/I based estimates when TOVS data especially over deserts (Prigent et al, 1998), where the TOVS product is generally missing, and climatology is used.

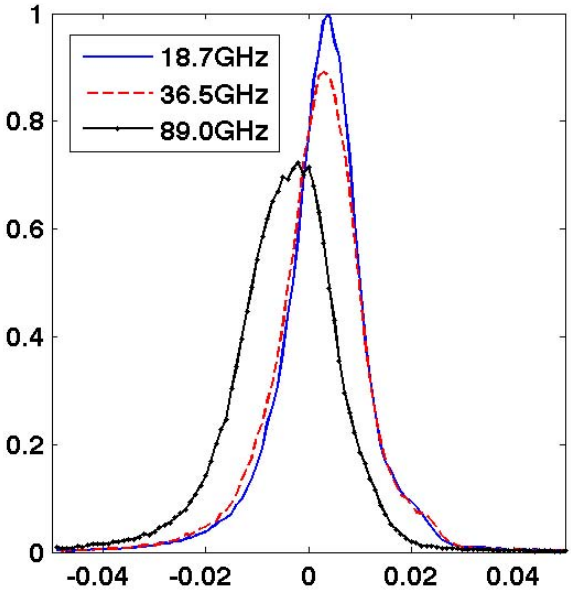

Fig. 1. Normalized histogram of the difference between SSM/I and AMSR-E products at close to 18.7, 36.5, and 89.0 GHz (horizontal polarization) for July 2003.

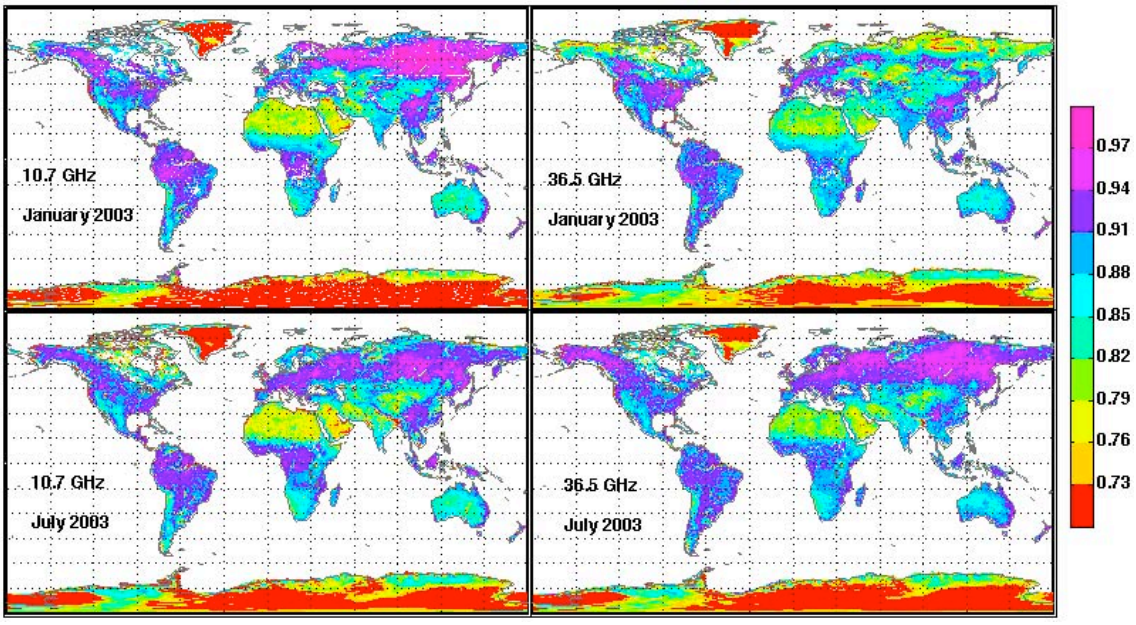

Fig. 2. Composite monthly mean land surface emissivity at 10.7, and 36.5 GHz (horizontal polarization) for January and July 2003.

4 Results and discussion

Cloud-free AMSR-E brightness temperatures from June 2002 through June 2008 are used to globally retrieve land surface emissivities. The ISCCP cloud mask indicates that, on average, more than 50 % (monthly average) of the land, is cloud covered (Rossow and Schiffer, 1999), which significantly limits the instantaneous spatial coverage. In addition, gaps between consecutive orbit swaths induce further loss of data and reduce the coverage. The instantaneous coverage of the product varies between 25 and 35 % depending on the season.

4.1 Land emissivity and surface physical properties

Examples of monthly mean composites of estimated land emissivities for January and July 2003 for horizontal polarization at 10.7 and 36.5 GHz are presented in Fig. 2. For relatively smooth bare soils, land surface emissivity is smaller in horizontal polarization compared to vegetated areas. For instance, in North Africa and Saudi Arabia, which are mostly dominated by bare soils and desert, a noticeably smaller emissivity can be seen compared to highly vegetated regions such as Amazon or Congo, which exhibit relatively larger emissivities. Generally, the 10.7 GHz shows smaller emissivity values in arid and semi-arid regions (North Africa and Australian Desert) compared with the same locations at 36.5 GHz. This is also observed in Australia, where smaller emissivities are obtained in deserts, whereas the vegetated western coast shows larger horizontal emissivity values. Fig. 2 shows emissivity estimates from microwave temperature at horizontal polarization which show opposite behavior when compared to estimates from vertical polarization observation, with the largest emissivity values found in desert areas. This behavior is due to the different responses of horizontal and vertical polarization emissivities to the dielectric constant (Njoku and Li, 1999; Owe et al., 2001). Also, seasonal variation of emissivity can be seen at some places such as in Russia where the 10.7 and 36.5 GHz show large differences in January and July with changes in land and snow covers. The seasonal variations of land surface emissivities with land cover change are discussed later.

The radiative properties of vegetation-covered surfaces are controlled by the dielectric properties of the vegetation components, their density, and the relative size of the vegetation components with respect to wavelength. As the surface roughness and wetness decrease, the polarization difference increases (Choudhury, 1989). As vegetation density increases the surface roughness also increases, which causes more scattering of microwave radiation. Figure 3 shows that most vegetated areas have polarization differences less than 2%. The largest polarization difference is observed in arid and semi-arid regions such as North Africa. The polarization difference at 6.9 GHz in these regions is systematically larger than at 89.0, which can be attributed to greater relative size of desert roughness to wavelength at 89.0 GHz. Bare soil is rougher for observations at higher frequencies, as the relative size of the surface to the wavelength and the scattering are greater. This higher sensitivity to soil roughness at higher frequencies in desert areas causes larger polarization differences at lower frequencies in desert areas (Prigent et al., 2001).

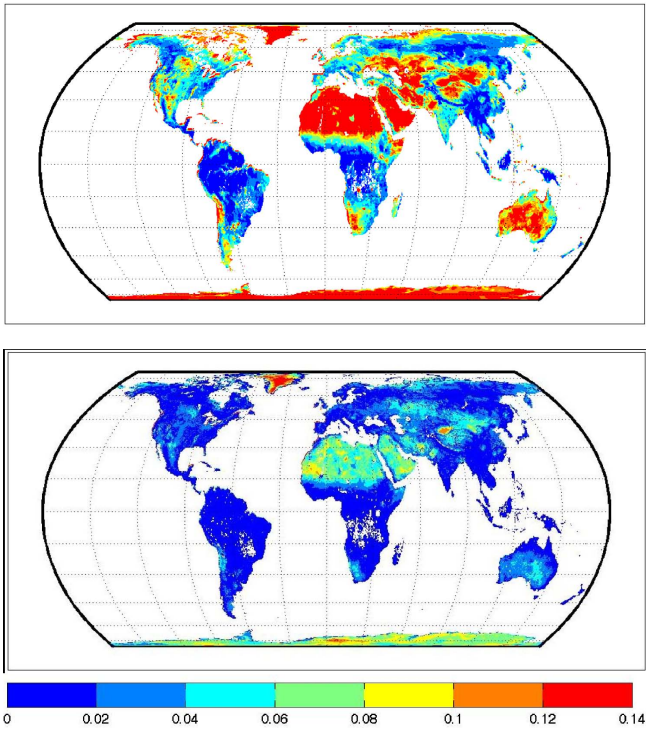

Fig. 3. Difference between vertical and horizontal polarizations land surface emissivity at 6.9 GHz (top), and 89.0 GHz (bottom) for January 2003.

Figure 4 shows the temporal variations of Northern and Southern Hemisphere monthly mean polarization differences at different frequencies for desert, deciduous woodland and rain forest areas, based on the vegetation classification introduced in (Matthews, 1983). As expected, the difference between horizontal and vertical polarization emissivity decreases with increasing frequency. The polarization gradient is larger at 6.9 GHz than at 89.0 GHz in all land classes (most not shown). Deserts have larger polarization differences but smaller interannual variability, since in arid regions the seasonal variation of soil moisture and vegetation cover is not significant (Fig. 4a, b). Most of the frequencies confirm this small seasonal variation in desert areas, except 89.0 GHz, which may include some residual atmospheric perturbations in the emissivity retrieval. However, vegetated areas (for example deciduous woodland areas) show smaller polarization differences with larger seasonal variations that correspond to variations in vegetation density (Fig. 4c, d). In places with constant high-density vegetation, such as rain forest, the polarization differences exhibit almost no seasonal variation (Fig. 4e, f), as the change of the land cover is not significant. This polarization difference can be considered as an indicator of land cover and vegetation type, as the polarization difference decreases with increasing vegetation density.

The relationship between the retrieved land surface emissivity and physical properties, such as Normalized Difference Vegetation Index (NDVI) and soil moisture content, is investigated to assess the sensitivity of lower frequency emissivities to these parameters. The comparison between monthly average (July 2005) global emissivity polarization difference (V-H) at 6.9 and 10.7 GHz and NDVI values from MODIS observations distributed by the Land Processes Distributed Active Archive Center (LP DAAC) is displayed in Fig. 5a, b. Note that y-axis in this scatter plot is logarithmic to make the relationship clearer. The peak frequency of pixels occurs at small NDVI and large (logarithm of) emissivity differences. In general, the emissivity polarization difference decreases as NDVI increases. However, at larger NDVI values in high density vegetated regions, the correlations between emissivity polarization difference and NDVI are much lower. The regions with NDVI greater than 0.6 show different structures than NDVI less than 0.6 with respect to emissivity in Fig. 5a and b. It was found that these regions with NDVI greater than 0.6 and greater emissivity belong to regions that are flooded or in coastal regions. These regions also showed significant seasonal variation. Figure 5c and d illustrate the emissivity polarization differences at 6.9 and 10.7 GHz versus the soil moisture product from the Advanced Scatterometer (ASCAT) provided by the European Organization for the Exploitation of Meteorological Satellites (EUMETSAT) (Bartalis et al., 2008). The correlation between log of emissivity polarization differences at 10.7 GHz and soil moisture content is less than 70 % and is 71 % at 6.9 GHz. Weaker correlations (between 65 % to 70 %) were found at higher frequencies (higher than 19 GHz) (not displayed). As soil moisture increases the logarithm of emissivity difference decreases. One should note that soil moisture and NDVI are interrelated which may be the reason for the similar relationship between emissivity and these parameters (Prigent et al., 2005).

The agreement between monthly variations of NDVI and (H-V) emissivity polarization difference at 10.7 GHz for each pixel at global scale was analyzed for the period from January 2003 through December 2007. The results shown in Fig. 6 confirm that correlation of emissivity monthly variation with vegetation density variation is very small in desert areas (North Africa; Saudi Arabia) and in densely vegetated area such as Amazon and Congo basins. In predominantly vegetated areas emissivity may be sensitive to other physical parameters such as vegetation water content. In densely vegetated areas, emissivity is less sensitive to soil moisture. However, it is difficult to accurately distinguish between the effects of soil moisture and vegetation on land emissivity and its polarization difference, as the determination of the exact relationship between these parameters and emissivity is not fully comprehended (Aires et al., 2005; Prigent et al., 2005, 2001). It is also worth noting that NDVI in Tropical regions could have some cloud contaminations because of the persistency of cloudy conditions in these regions. This may reduce the correlation between NDVI and emissivity polarization difference.

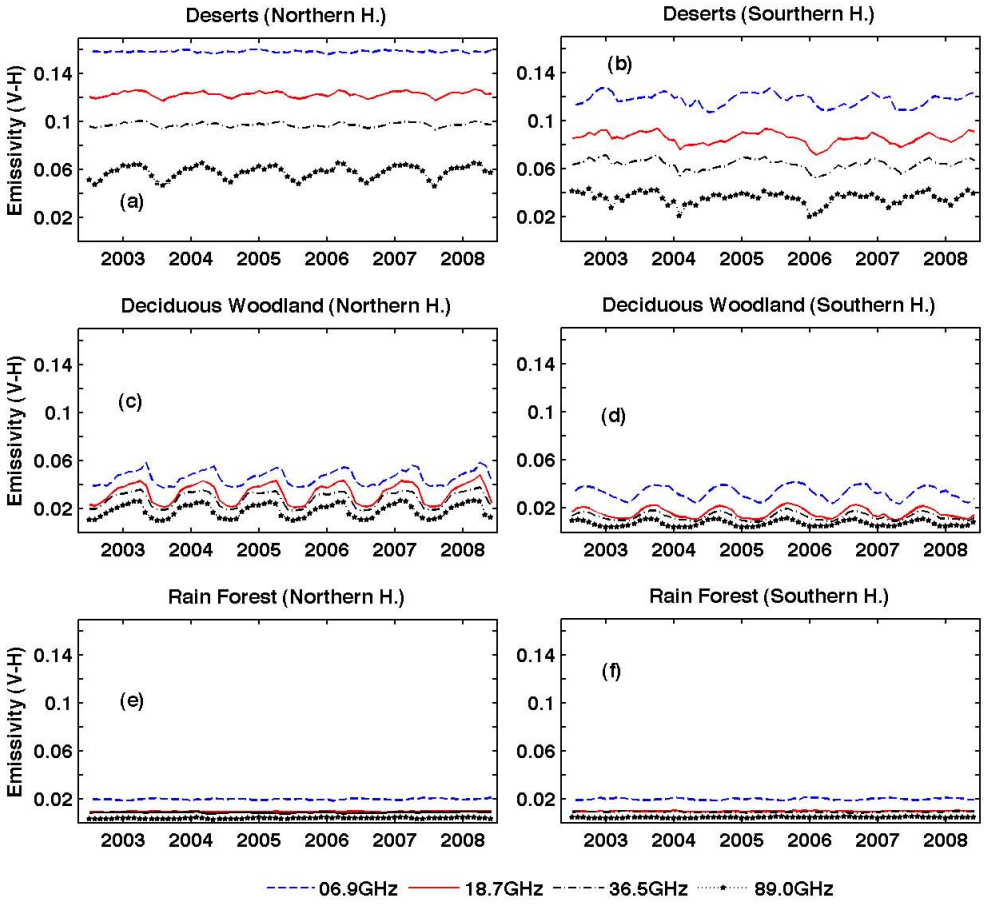

Fig. 4. Seasonal variation of the vertical and horizontal polarization differences at 6.9, 18.7, 36.5, and 89.0 GHz in **(a, b)** desert regions **(c, d)** deciduous woodland **(e, f)** rain forest (Matthew's vegetation classification (Matthews, 1983) for Northern and Southern Hemisphere.

The monthly variation of emissivity polarization differences at 10.7 GHz H-V (not V-H) and those of NDVI and soil moisture at different locations is also examined. A selection of results is shown in Fig. 7 for different regions with moderate vegetation and large seasonal variation (densely vegetated and desert areas show low correlations with monthly variation of emissivity polarization difference). In general, they show a good agreement as they display similar monthly variation with correlation coefficients of more than 0.9. At some places, such as Lat = 15° S and Lon = 30° E (Fig. 7a), the polarization difference shows better agreement with NDVI variations. This region is at the edge of the North African Desert and the effect of soil moisture changes is amplified by the seasonal variation of vegetation, so there is a stronger relationship with the emissivity difference. This might indicate that the soil moisture signal does not persist as the vegetation signal does as soil moisture tend either to evaporate or infiltrate more rapidly and does not remain in top surface layers. Generally, soil moisture tends to precede NDVI and emissivity. However, in other regions farther to the south, such as Lat = 13° S and Lon = 20° E, soil moisture is more persistent, which produces better consistency with the variability of emissivity difference (H-V) (Fig. 7c). Overall, these features of the results indicate that the retrieval of low frequency emissivity is consistent with known properties of the surface, such as soil moisture and vegetation structure.

4.2 Emissivity variability/ascending and descending differences

The day-to-day variability of emissivity at different frequencies is represented by the daily mean values (ascending and descending) to test the stability of the retrieval. It means the average of emissivity from both ascending and descending emissivities is calculated for each day. Then, the standard deviation of daily averaged emissivities (vertical polarization) for July 2003 is shown in Table 2 for different land cover types based on (Matthews, 1983). The RMS variability is less than 0.021, which demonstrates the consistency of the instantaneous emissivity product on monthly time scales. We assume that the geophysical properties of the land surface (such as vegetation cover) do not change dramatically on this

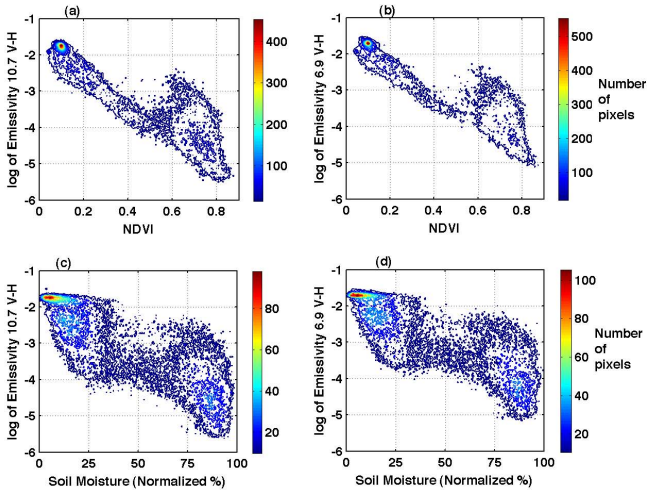

Fig. 5. (a–b) Scatter plot of logarithm of emissivity polarization difference at 10.7 GHz and 6.9 GHz (V-H) versus NDVI. **(c–d)** Scatter plot of logarithm of emissivity polarization difference at 10.7 GHz and 6.9 GHz (V-H) versus ASCAT soil moisture.

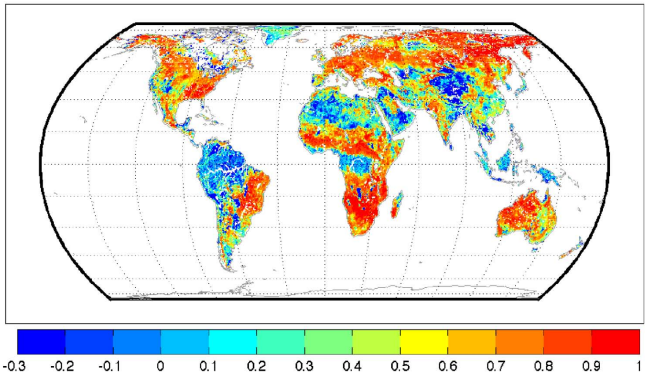

Fig. 6. Map of correlation between monthly variation (time series) of emissivity polarization difference at 10.7 GHz (H-V) and NDVI monthly mean variation for time period of January 2003 to December 2007.

time scale, although vegetation, soil moisture, snow cover can change within a month, especially in transition zones and seasons. Table 2 also shows that as vegetation density decreases, the day-to-day variability increases. The largest standard deviations of about 0.02 are seen in the desert areas and the smallest values around 0.01 occur in rain forest or densely vegetated regions. In desert regions, the day-to-day variability mostly decreases, while in densely vegetated areas the standard deviation increases as the frequency increases. In desert areas, this could be due to less difference between the surface skin temperature and the effective emitting temperature. The increase of the variability in vegetated areas can be due to larger atmospheric effect.

The difference between the retrieved emissivities from the ascending and descending parts of the orbits (day and night)

Table 2. Day to day variability of global mean emissivity at vertical polarization for July 2003 at different land vegetation covers.

	Day to day variability				
Land Class Type	6.9 GHz	10.7 GHz	18.7 GHz	36.5 GHz	89 GHz
Rain forest	0.0092	0.0093	0.0096	0.0103	0.0112
Evergreen forest	0.0107	0.0105	0.0109	0.0113	0.0136
Deciduous forest	0.0110	0.0106	0.0106	0.0111	0.0141
Evergreen woodland	0.0162	0.0148	0.0148	0.0148	0.0179
Deciduous woodland	0.0191	0.0179	0.0175	0.0173	0.0189
Cultivation	0.0148	0.0140	0.0133	0.0132	0.0154
Grassland	0.0190	7 0.0176	0.0167	0.0163	0.0187
Tundra	0.0175	0.0168	0.0158	0.0173	0.0233
Shrub land	0.0198	0.0180	0.0170	0.0164	0.0191
Desert	0.0249	0.0232	0.0212	0.0197	0.0218

is shown in Fig. 8 for 10.7 GHz and 89.0 GHz horizontal polarization (as representatives of lower and higher frequencies). The average of the descending passes was subtracted from the average of ascending passes to generate these maps. Large differences occur in desert and mountainous locations even though we expect less difference because of small moisture changes from day to night. These maps are for July 2003, however we also found similar differences in other months to what is presented here. These differences are more than 0.1 in some regions such as North Africa, and are much larger than emissivity variability in available SSM/I product with standard deviation of about 0.02. This larger systematic difference than seen in SSM/I results can be explained by the timing of the overpass: since the daytime overpass is closer to the daily maximum temperature but the nighttime pass is not near to the daily minimum temperature. The difference of diurnal temperature cycle phase will be larger during daytime than nighttime (Grody and Weng, 2008; Prigent et al., 1999). For some surface types, such as sand dunes, the microwave signal comes from a deeper layer than the surface with a different diurnal temperature amplitude and phase than the surface (Prigent et al., 1999). Using the IR skin temperature in the emissivity retrieval causes this inconsistency. The fact that this inconsistency is even larger for the lower AMSR-E frequencies corroborates previous findings that microwave emission at lower frequencies is generated from deeper soil layers. The lack of global soil temperature profiles makes removing this inconsistency challenging especially in arid regions. This effect is more pronounced in AMSR-E than SSM/I observations because they occur closer to the extremes of the diurnal temperature cycle. 10.7 and 89.0 GHz both have the same pattern of differences; but the emissivity difference between day and night at 89.0 GHz is noticeably smaller than 10.7 GHz at the same locations such as North and South Africa, due to small penetration depth of 89.0 GHz. A map that shows the effect of penetration depth in North Africa and Arabian Peninsula was produced by Prigent et al. (1999). The comparison between this map and the emissivity difference map during day and night (Fig. 8)

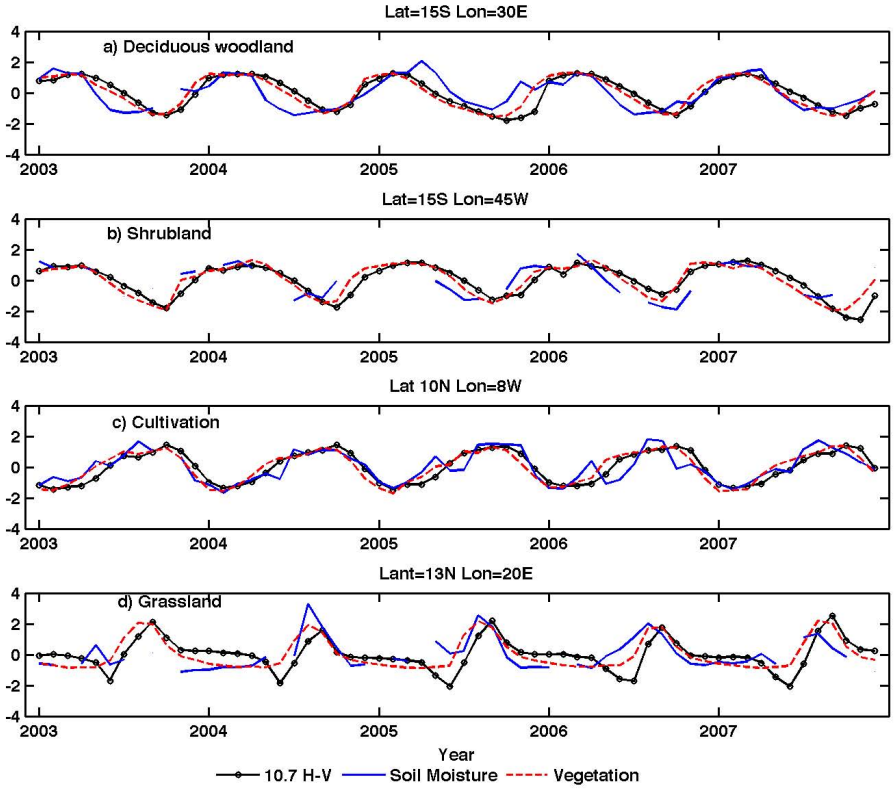

Fig. 7. (a–d) Normalized monthly mean variation of emissivity polarization difference at 10.7 GHz (H-V), NDVI, and soil moisture content at different locations from January 2003 to December 2007. The vegetation types of these locations are **(a)** deciduous woodland **(b)** shrubland **(c)** cultivation **(d)** grassland.

reveals an overall consistency, despite some differences noticed in western part of Sahara Desert. These discrepancies will be carefully examined in subsequent studies, but we would expect to see some penetration effect over a wider area because the diurnal temperature contrasts are larger for the AMSR-E overpass times than for the SSM/I overpass times. We also found similar differences at horizontal polarization.

4.3 Discussion

Retrieval of land surface emissivity from different sensors and at different frequencies helps to understand the properties of land surface. Previous studies have shown that land surface emissivity can be used to classify the land cover using the difference between horizontal and vertical polarization emissivity (Prigent et al., 2001). Using two even lower frequency emissivities (C- and X-bands) can describe land cover variations in more details because of their greater sensitivity to the subsurface. Polarization differences, especially at lower frequencies, can be interpreted as a roughness effect. As the vegetation increases, the roughness increases and decreases the difference between emissivities at horizontal and vertical polarization. These patterns may be used to quantify the polarization difference for land cover classification/vegetation detection (Prigent et al., 2001).

However, there are some difficulties in emissivity retrieval at lower frequencies. Significant differences in the emissivity maps between the ascending and descending overpasses were noticed particularly in deserts. The effect of the temperature diurnal cycle amplitude and phase lag between the microwave and infrared temperatures needs further investigation and should be accounted for in future retrieval procedures. More similarity in term of penetration depth between the higher passive microwave frequencies and thermal wavelengths should produce more nearly synchronous brightness temperature and thermal skin temperature diurnal cycles, but at lower frequencies the microwave signal is sensitive to deeper soil layers (on the order of few centimeters at the L-band) (Grody and Weng, 2008). This leads to a lag between the diurnal variations of the skin temperature and brightness temperature and inaccurate emissivity values. This issue is worse for AMSR-E observations because of its unique overpass time at early morning and maximum temperature of the day. However, the other sensors are providing more consistent results than AMSR-E in this respect, even though they show larger emissivity variability. Therefore, mitigating these discrepancies for AMSR-E emissivity estimates sounds necessary. Revising the skin temperature in order to infer an effective temperature that is representative of the deeper layer in the soil could resolve this inconsistency.

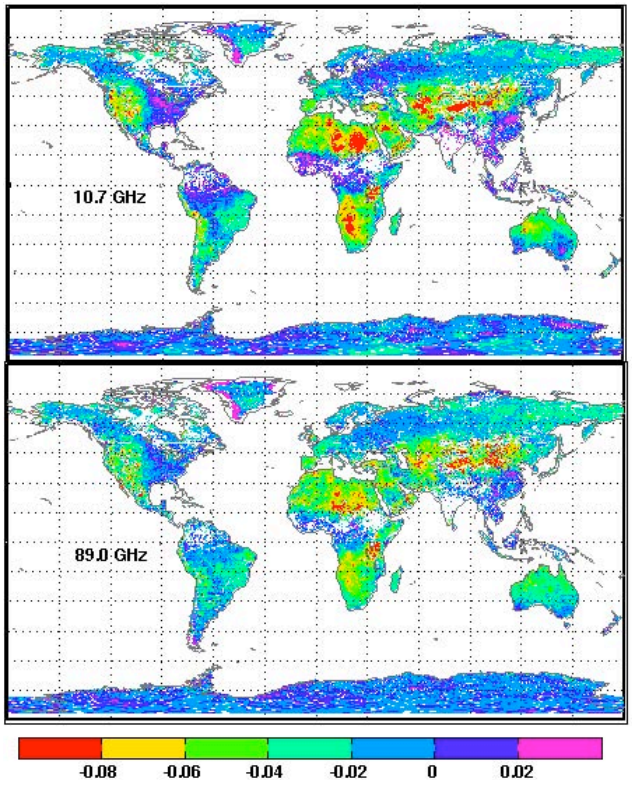

Fig. 8. Difference between ascending and descending monthly mean of AMSR-E emissivity at 10.7 GHz (top), and 89.0 GHz (bottom) in horizontal polarization for July 2003.

5 Conclusions

A procedure using multi-satellite observations for retrieving instantaneous land surface emissivities from AMSR-E observations under clear sky conditions at all frequencies and both polarizations is tested. Monthly mean composite maps are produced at all frequencies and polarizations for more than six years. The results compared with previous studies show reasonable consistency. The remaining differences, after accounting for the differences due to the geometry and frequency, can be explained mostly by the difference in overpass times between two different sensors (AMSR-E and SSM/I). The methodology is general and extendable to other sensors, such as WindSat, to achieve better temporal and spatial coverage. In this study, the focus was on the potential and difficulties of retrieval at the two lower frequency emissivities that can be obtained from AMSR-E. Differences between the vertical and horizontal polarizations at C- and X-band were in good qualitative agreement with known variations of vegetation density and surface roughness and can be used as additional indicators of land cover or vegetation type variation at global scales. Large correlations were found in moderately vegetated areas with the large seasonal variations of the lower frequencies polarization differences and physical properties such as soil moisture and vegetation density (represented by NDVI). The seasonal variations of the polarization difference may be used to quantify changes in vegetation density and potentially crop yield.

The difference between day and night emissivities was also examined. The lower the frequency is, the larger the difference would be. This can be explained by the difference between the skin temperature diurnal variations (amplitude and phase) and the temperature variations at the differing penetration depths for different frequencies. This effect is especially larger for AMSR-E because its overpass times are closer to the daily extremes of the skin temperature. A method is needed to account for this inconsistency between infrared thermal temperature and microwave brightness temperatures to remove the differences between emissivities at ascending and descending overpasses.

The results of this study may be extended to L band (about 1.4 GHz), which has been found to be more suitable for soil moisture retrieval. Such measurements are available since 2010 from the Soil Moisture and Ocean Salinity (SMOS) mission (Jorda et al., 2011). In 2014, Soil Moisture Active and Passive (SMAP) mission will be launched (Entekhabi et al., 2010) and will also provide us with emissivity estimates at L-band to complement those obtained from AMSR-E.

Acknowledgements. This study was partially supported by National Oceanic and Atmospheric Administration (NOAA) under grant NA06OAR4810162, NASA Energy and Water Study (NEWS) under grant NNXD7AO90G, and the City University of New York graduate center. The MODIS NDVI data are distributed by the Land Processes Distributed Active Archive Center (LP DAAC), located at the US Geological Survey (USGS) Earth Resources Observation and Science (EROS) Center (lpdaac.usgs.gov). The authors would like to thank Catherine Prigent, Fabrice Papa, the editor Alexander Loew, and reviewers for their fruitful discussion and comments on this paper.

Edited by: A. Loew

References

Aires, F., Prigent, C., and Rossow, W. B.: Temporal interpolation of global surface skin temperature diurnal cycle over land under clear and cloudy conditions, J. Geophy. Res.-Atmos., 109, D04313, doi:10.1029/2003jd003527, 2004.

Aires, F., Prigent, C., and Rossow, W. B.: Sensitivity of satellite microwave and infrared observations to soil moisture at a global scale: 2. Global statistical relationships, J. Geophy. Res.-Atmos., 110, D07110, doi:10.1029/2004jd005094, 2005.

Bartalis, Z., Naeimi, V., Hasenauer, S., and Wagner, W.: Ascat soil moisture product guide, ASCAT Soil Moisture Report Series, No. 15, 2008.

Choudhury, B. J.: Monitoring global land surface using nimbus-7 37 GHz data theory and examples, Int. J. Remote Sens., 10, 1579–1605, 1989.

Choudhury, B. J.: Reflectivities of selected land-surface types at 19 and 37 GHz from ssm/i observations, Remote Sens. Environ., 46, 1–17, 1993.

English, S. J.: Airborne radiometric observations of cloud liquid-water emission at 89 and 157 GHz – application to retrieval of liquid-water path, Q. J. Roy. Meteor. Soc., 121, 1501–1524, 1995.

Entekhabi, D., Njoku, E. G., O'Neill, P. E., Kellogg, K. H., Crow, W. T., Edelstein, W. N., Entin, J. K., Goodman, S. D., Jackson, T. J., Johnson, J., Kimball, J., Piepmeier, J. R., Koster, R. D., Martin, N., McDonald, K. C., Moghaddam, M., Moran, S., Reichle, R., Shi, J. C., Spencer, M. W., Thurman, S. W., Tsang, L., and Van Zyl, J.: The soil moisture active passive (smap) mission, Proc. IEEE, 98, 704–716, doi:10.1109/jproc.2010.2043918, 2010.

Grody, N. C. and Weng, F.: Microwave emission and scattering from deserts: Theory compared with satellite measurements, IEEE, T. Geosci. Remote, 46, 361–375, doi:10.1109/tgrs.2007.909920, 2008.

Jimenez, C., Prigent, C., Mueller, B., Seneviratne, S. I., McCabe, M. F., Wood, E. F., Rossow, W. B., Balsamo, G., Betts, A. K., Dirmeyer, P. A., Fisher, J. B., Jung, M., Kanamitsu, M., Reichle, R. H., Reichstein, M., Rodell, M., Sheffield, J., Tu, K., and Wang, K.: Global intercomparison of 12 land surface heat flux estimates, J. Geophy. Res.-Atmos., 116, D02102, doi:10.1029/2010jd014545, 2011.

Jones, A. S. and VonderHaar, T. H.: Retrieval of microwave surface emittance over land using coincident microwave and infrared satellite measurements, J. Geophy. Res.-Atmos., 102, 13609–13626, 1997.

Jones, A. S., Vukicevic, T., and Vonder Haar, T. H.: A microwave satellite observational operator for variational data assimilation of soil moisture, J. Hydrometeorol., 5, 213–229, 2004.

Jones, L. A., Kimball, J. S., McDonald, K. C., Chan, S. T. K., Njoku, E. G., and Oechel, W. C.: Satellite microwave remote sensing of boreal and arctic soil temperatures from amsr-e, IEEE, T. Geosci. Remote, 45, 2004–2018, doi:10.1109/tgrs.2007.898436, 2007.

Jorda, G., Gomis, D., and Talone, M.: The smos l3 mapping algorithm for sea surface salinity, IEEE, T. Geosci. Remote, 49, 1032–1051, doi:10.1109/tgrs.2010.2068551, 2011.

Kalnay, E., Kanamitsu, M., Kistler, R., Collins, W., Deaven, D., Gandin, L., Iredell, M., Saha, S., White, G., Woollen, J., Zhu, Y., Chelliah, M., Ebisuzaki, W., Higgins, W., Janowiak, J., Mo, K. C., Ropelewski, C., Wang, J., Leetmaa, A., Reynolds, R., Jenne, R., and Joseph, D.: The ncep/ncar 40 yr reanalysis project, B. Am. Meteorol. Soc., 77, 437–471, 1996.

Karbou, F., Aires, F., Prigent, C., and Eymard, L.: Potential of advanced microwave sounding unit-a (amsu-a) and amsu-b measurements for atmospheric temperature and humidity profiling over land, J. Geophy. Res.-Atmos., 110, D07109, doi:10.1029/2004jd005318, 2005a.

Karbou, F., Prigent, C., Eymard, L., and Pardo, J. R.: Microwave land emissivity calculations using amsu measurements, IEEE, T. Geosci. Remote, 43, 948–959, doi:10.1109/tgrs.2004.837503, 2005b.

Karbou, F., Gerard, E., and Rabier, F.: Microwave land emissivity and skin temperature for amsu-a and -b assimilation over land, Q. J. Roy. Meteor. Soc., 132, 2333–2355, doi:10.1256/qj.05.216, 2006.

Kawanishi, T., Sezai, T., Ito, Y., Imaoka, K., Takeshima, T., Ishido, Y., Shibata, A., Miura, M., Inahata, H., and Spencer, R. W.: The advanced microwave scanning radiometer for the earth observing system (amsr-e), nasda's contribution to the eos for global energy and water cycle studies, IEEE, T. Geosci. Remote, 41, 184–194, doi:10.1109/tgrs.2002.808331, 2003.

Li, L., Gaiser, P. W., Bettenhausen, M. H., and Johnston, W.: Windsat radio-frequency interference signature and its identification over land and ocean, IEEE, T. Geosci. Remote, 44, 530–539, doi:10.1109/tgrs.2005.862503, 2006.

Liebe, H. J., Hufford, G. A., and Cotton, M. G.: Propagation modelling of moist air and suspended water/ice particles at frequencies below 1000 GHz, presented at the Specialist Meeting of the Electromagnetic Wave Propagation Panel Symposium, AGARD Conference Proceedings 542, Atmospheric propagation effects through natural and man-made obscurants for visible through MW-wave radiation, 3-1–3-10, Palma de Mallorca, Spain, 1993,

Lin, B., and Rossow, W. B.: Observations of cloud liquid water path over oceans – optical and microwave remote-sensing methods, J. Geophy. Res.-Atmos., 99, 20907–20927, 1994.

Matthews, E.: Global vegetation and land-use data-bases for climate studies, B. Am. Meteorol. Soc., 64, 793–794, 1983.

Min, Q. L., Lin, B., and Li, R.: Remote sensing vegetation hydrological states using passive microwave measurements, IEEE J. Sel. Top. Appl., 3, 124–131, doi:10.1109/jstars.2009.2032557, 2010.

Moncet, J., Liang, P., Galantowicz, A., Lipton, A., Uymin, G., Prigent, C., and Grassotti, C.: Land surface microwave emissivities derived from amsr-e and modis measurements with advanced quality control, J. Geophy. Res.-Atmos., 116, D16104, doi:10.1029/2010JD015429, 2011a.

Moncet, J., Liang, P., Lipton, A., Galantowicz, J., and Prigent, C.: Discrepancies between MODIS and ISCCP land surface temperature products analyzed with microwave measurements, J. Geophys. Res., 116, D21105, doi:10.1029/2010JD015432, 2011B.

Njoku, E. G. and Li, L.: Retrieval of land surface parameters using passive microwave measurements at 6–18 GHz, IEEE, T. Geosci. Remote, 37, 79–93, 1999.

Njoku, E. G., Jackson, T. J., Lakshmi, V., Chan, T. K., and Nghiem, S. V.: Soil moisture retrieval from amsr-e, IEEE, T. Geosci. Remote, 41, 215-229, 10.1109/tgrs.2002.808243, 2003.

Njoku, E. G., Ashcroft, P., Chan, T. K., and Li, L.: Global survey and statistics of radio-frequency interference in amsr-e land observations, IEEE, T. Geosci. Remote, 43, 938–947, doi:10.1109/tgrs.2004.837507, 2005.

Owe, M., de Jeu, R., and Walker, J.: A methodology for surface soil moisture and vegetation optical depth retrieval using the microwave polarization difference index, IEEE, T. Geosci. Remote, 39, 1643–1654, 2001.

Prigent, C., Rossow, W. B., and Matthews, E.: Microwave land surface emissivities estimated from ssm/i observations, J. Geophy. Res.-Atmos., 102, 21867–21890, 1997.

Prigent, C., Rossow, W. B., and Matthews, E.: Global maps of microwave land surface emissivities: Potential for land surface characterization, Radio Sci., 33, 745–751, 1998.

Prigent, C., Rossow, W. B., Matthews, E., and Marticorena, B.: Microwave radiometric signatures of different surface types in deserts, J. Geophy. Res.-Atmos., 104, 12147–12158, 1999.

Prigent, C., Aires, F., Rossow, W., and Matthews, E.: Joint characterization of vegetation by satellite observations from visible to microwave wavelengths: A sensitivity analysis, J. Geophy. Res.-Atmos., 106, 20665–20685, 2001.

Prigent, C., Aires, F., Rossow, W. B., and Robock, A.: Sensitivity of satellite microwave and infrared observations to soil moisture at a global scale: Relationship of satellite observations to in situ soil moisture measurements, J. Geophy. Res.-Atmos., 110, D07110, doi:10.1029/2004jd005087, 2005.

Prigent, C., Aires, F., and Rossow, W. B.: Land surface microwave emissivities over the globe for a decade, B. Am. Meteorol. Soc., 87, 1573–1584, doi:10.1175/bams-87-11-1573, 2006.

Prigent, C., Jaumouille, E., Chevallier, F., and Aires, F.: A parameterization of the microwave land surface emissivity between 19 and 100 GHz, anchored to satellite-derived estimates, IEEE, T. Geosci. Remote, 46, 344–352, doi:10.1109/tgrs.2007.908881, 2008.

Rossow, W. B. and Schiffer, R. A.: Isccp cloud data products, B. Am. Meteorol. Soc., 72, 2–20, 1991.

Rossow, W. B. and Schiffer, R. A.: Advances in understanding clouds from isccp, B. Am. Meteorol. Soc., 80, 2261–2287, 1999.

Tedesco, M., and Kim, E. J.: Retrieval of dry-snow parameters from microwave radiometric data using a dense-medium model and genetic algorithms, IEEE, T. Geosci. Remote, 44, 2143–2151, doi:10.1109/tgrs.2006.872087, 2006.

Weng, F. Z.: Advances in radiative transfer modeling in support of satellite data assimilation, J. Atmos. Sci., 64, 3799–3807, doi:10.1175/2007jas2112.1, 2007.

Weng, F. Z., Yan, B. H., and Grody, N. C.: A microwave land emissivity model, J. Geophy. Res.-Atmos., 106, 20115–20123, 2001.

Zhang, L. X., Zhao, T. J., Jiang, L. M., and Zhao, S. J.: Estimate of phase transition water content in freeze-thaw process using microwave radiometer, IEEE, T. Geosci. Remote, 48, 4248–4255, doi:10.1109/tgrs.2010.2051158, 2010.

Zhang, Y. C., Rossow, W. B., and Stackhouse, P. W.: Comparison of different global information sources used in surface radiative flux calculation: Radiative properties of the near-surface atmosphere, J. Geophy. Res.-Atmos., 111, D13106, doi:10.1029/2005jd006873, 2006.